
Article:
Wei, X, Zhang, P, Wei, D et al. (3 more authors) (2017) Mechanical and tribological properties of Cr-Nb double-glow plasma coatings deposited on TiAl alloy. Tribology - Materials, Surfaces & Interfaces, 11 (2). pp. 98-106. ISSN 1751-5831

https://doi.org/10.1080/17515831.2017.1339484

Mechanical and tribological properties of Cr-Nb double-glow plasma coatings deposited on TiAl alloy

Xiangfei Wei [a, *], Pingze Zhang [a], Dongbo Wei [a], Hongyuan Zhao [b], Chun Wang [b], Tomasz Liskiewicz [b]

[a] College of Materials Science and Technology, Nanjing University of Aeronautics and Astronautics, Nanjing, 211106, China.

[b] School of Mechanical Engineering, University of Leeds, Leeds, LS2 9JT, UK.

*Corresponding author: wxf1018@nuaa.edu.cn

Abstract: Double glow plasma (DGP) coatings are recommended for metallic components to mitigate the damage induced by complex working conditions in previous studies. In this paper, Nb-rich ($CrNb_4$) and Cr-rich (Cr_4Nb) alloyed layers were formed onto the TiAl substrate via a DGP process to enhance its wear resistance. Scratch and Nano-indentation tests were used to evaluate the mechanical properties of the coatings. The tribological behavior of the coatings were investigated using a pin-on-disc tribometer by rubbing against the GCr15 ball. Results from surface analysis techniques showed that the coatings mainly comprised Cr, Nb, and Cr_2Nb phases, and were well bonded to the substrate. The hardness of the $CrNb_4$ coating was 11.61GPa and the Cr_4Nb coating was 9.66 GPa which all higher than that of the uncoated TiAl which was 5.65 GPa. However, the critical load of the Cr_4Nb coating ~21.64 was higher than that of the $CrNb_4$ coating ~17.6. And the specific wear rate of $CrNb_4$ coating, Cr_4Nb coating and uncoated TiAl were 3.54×10^{-4}, 0.01×10^{-4} and $1.53\times10^{-4}mm^3N^{-1}m^{-1}$ respectively. The low-wear mechanism of the coatings is discussed in detail in this paper.

Keywords: TiAl; Double glow plasma; Nano-indentation; Friction; Chromium-Niobium.

1 Introduction

The TiAl intermetallic alloy has been widely used as one of the potential materials in variety of industrial fields, such as, motor, energy and aerospace industry, due to their high specific stiffness and strength as well as creep and oxidation resistance[1, 2]. The application of TiAl alloys in aero-engine would be beneficial to weight reducing of machine parts and the enhancing of thrust load[3]. Nevertheless, the low hardness and poor wear resistance of the TiAl intermetallic becomes a principal obstacle for application ranges. Wear damage occurs with counterface materials due to fatigue, especially in complex situation of aerospace field[4]. So far, there are two ways to improve the tribological properties of TiAl. One is by smelting to change alloy composition, like add Cr, Nb, Si, W or other elements[5-7]. The other is by surface modification, like ion implantation[8], physical vapour deposition[9] and plasma nitriding[10]. The former technique changes the cast structure to improve the comprehensive mechanical properties of alloys, but sometimes, a number of interstitial elements doped in TiAl alloys are detrimental to ductility and increase the cost of products. Thus, surface modification, as an effective and economical method, has been paid more and more attention, and therefore, various coatings have been applied on TiAl alloys to improve the tribological properties, because the surface modification brings little effect on the mechanical performance of the alloy substrates.

The DGP surface alloying technique, known as Xu-Tec process in some literature[10], is an effective method to improve the micro-hardness, oxidation resistance and wear resistance of metals or alloys. In recent years, Coatings of Cr and Nb were used to improve the tribological properties of TiAl and that has obtained good achievement. Cr can replace Ti and Al position to reform Ti-Al-Cr compound to improve the hardness of the alloy, after a certain amount of Cr is added to TiAl alloy[11,

[12]. Nb has great capacity of alloying and can maintain good microstructure stability, and it can also form solid solution strengthening phase with Ti and Al to improve the stability of the alloy structure and high temperature strength[13].

In this study, Cr-Nb alloying layer was first deposited on TiAl substrate by DGP surface alloying technique. The microstructural morphology, phase composition and elements distribution of the modified layer were detected. And the friction and wear mechanisms under room temperature were analysed and discussed.

2 Experimental Procedures

2.1 Preparation of Materials

The casting TiAl alloy for this study was produced by induction shell melting and the chemical composition of this alloy is shown in Table 1. The ingot was cut into the plate size of 14mm × 14mm × 3mm. The TiAl alloy sample was used as the substrate material (the cathode). The Cr–Nb (Cr: Nb=1: 4 and Cr: Nb=4: 1, wt %) plate (80mm×5mm*15) was used as the target for supplying the alloying element (the source).

Table. 1 The chemical composition of the γ-TiAl alloy (wt %)

Ti	Al	V	Cr	Nb	O	C	N
Base	46.5	≤1.5	≤1	≤0.20	≤0.015	≤0.1	≤0.05

The schematic diagram of the double glow plasma surface alloying process is shown in Fig.1. The operating procedure of the DGP surface alloying technique is as follows[10]: the sample was placed on a platform inside a double walled, water-cooled vacuum chamber, and the anode and cathode were each connected to DC power supplies. The potential difference between the cathode and the source electrode resulted in an unequal potential, leading to the hollow cathode effect. Once the given voltage was applied, both the cathode and the source electrodes were surrounded by

the glow discharge. Cr-Nb ions were sputtered from the source electrode and deposited onto the substrate due to the bias gradient. With the bombardment of the ions, the desired alloying elements were sputtered from the source electrode, accelerated towards the sample and forced to diffuse into the sample's surface. The parameters of plasma Cr-Nb are shown in Table 2.

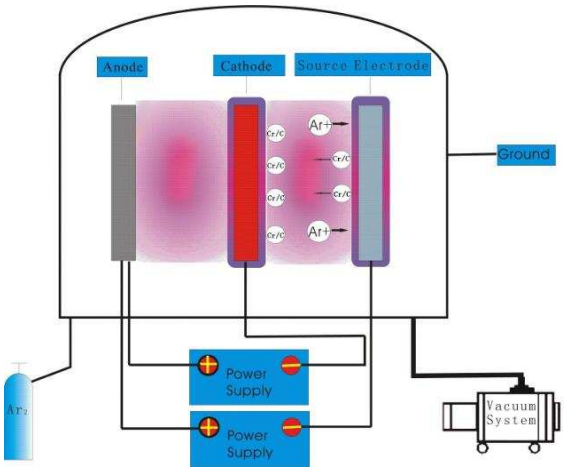

Fig. 1 Schematic diagram of DGP surface alloying technique.

Table. 2 Process parameters of plasma Cr-Nb.

Items	Plasma Cr-Nb
Processing temperature (°C)	900-950
Processing time (h)	3
Pressure (Pa)	30-40
Distance between source and cathode (mm)	18-20
Source voltage (V)	800-900
Cathode voltage (V)	500-600

2.2 Microstructure Analysis

The microstructure of Cr-Nb coated TiAl samples was investigated using a JSM-6360LV scanning electron microscope (SEM), and the alloying elements'

distribution was measured by an energy dispersive spectrometer (EDS). The phase composition of Cr-Nb alloyed layers was determined via Bruker D8-ADVANCE X-ray diffraction (XRD) with Cu K_α radiation over a range of 2θ from 20° to 90°.

2.3 Scratch tests

The scratch tests were performed by drawing a 0.2 mm radius Rockwell C diamond indenter across the coating surfaces under a normal load increasing linearly from 0 to 50 N which enables the measurement of mechanical strength adhesion and intrinsic cohesion of uncoated and Cr-Nb coated TiAl samples.

2.4 Nano-indentation tests

Nano-indentation tests were performed using a Micro-materials Nano-Test Platform® equipped with a Berkovich-type indenter, in order to measure the coating hardness and elastic modulus of the Cr-Nb coated TiAl samples.

The test was conducted by driving the indenture at a constant loading rate of 0.5mN s^{-1} into the sample's surface with the maximum applied load of 100 mN, as well as the holing time is 10 s and the maximum test depth is 1 μm (generally, the maximum depth of the indentation was no more than 10 % of the coating thickness[14]). In consideration of the accuracy and precision of the Nano-indentation tests, a minimum of five times parallel experiments were performed on each sample.

2.5 Sliding friction tests

Sliding friction tests were conducted on uncoated and Cr-Nb coated TiAl samples using an HT-500 ball-on-disk tribometer in air at room temperature (20°C± 4°C), and room relative humidity (45± 5 %) under dry sliding conditions. GCr15 balls with the average hardness of HRC63 and a diameter of 5 mm were used as the counterface material.

The tests were conducted at room temperature and at a constant angular speed of

10 Hz. A normal load of 4N and the test duration of 15min were used. The radius of rotating trajectory was 3 mm.

3 Results

3.1 Microstructure and phase composition

Fig. 2 shows the morphology and chemical composition of Cr-Nb coated Ti-Al samples. It can be seen that the surface of coatings appear as a dense and homogeneous structure without defects of porosity and cracks. And the contents of Cr and Nb in the $CrNb_4$ coating are 2.17 wt % and 97.40 wt %. The values are 61.46 wt % and 37.92 wt % respectively in the C_4Nb coating .

Fig. 3 illustrates the X-ray diffraction pattern of Cr-Nb coated Ti-Al samples. The composition of the $CrNb_4$ coating was consisted of Cr_2Nb and Nb phase (fig. 3(a)). On the other side the Cr_4Nb coating was consisted of Cr_2Nb and Cr phase (fig. 3(b)).

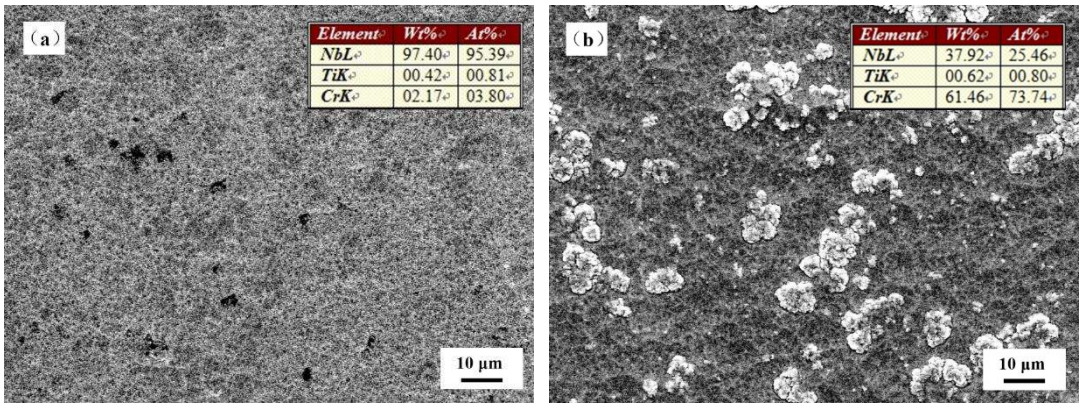

Fig. 2 Morphology and chemical composition of Cr-Nb coated TiAl samples (a) $CrNb_4$, (b) Cr_4Nb.

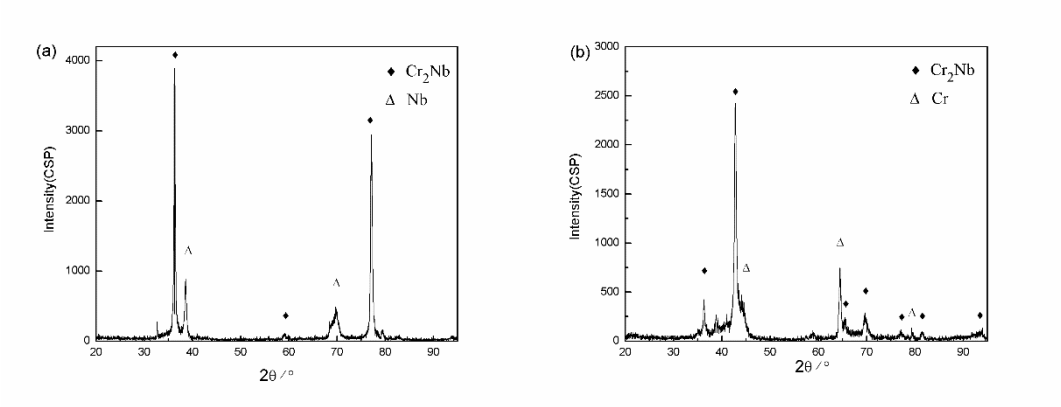

Fig. 3 XRD pattern of Cr-Nb coated TiAl samples (a) $CrNb_4$, (b) Cr_4Nb.

Fig. 4 shows the cross-section SEM image of Cr-Nb coated TiAl samples. It was evident that the Cr-Nb coated samples both exhibit a continuous and compact structure and are both well bonded to the γ-TiAl alloy. As shown in Fig. 5, line scan of cross sections are shown here, the coatings were all divided into two different areas, i.e., a deposition layer and a diffusion layer. The total depth of the $CrNb_4$ coating was about 18μm, consisting of Cr, Nb, Ti and Al elements. At the depth of 16 μm, the inter-diffusion layer was apparently observed, with about 2μm in thickness (fig 5(a)). As well as the total depth of the Cr_4Nb coating was about 8μm with the thickness of the interdiffusion layer about 2μm (fig 5(b)).

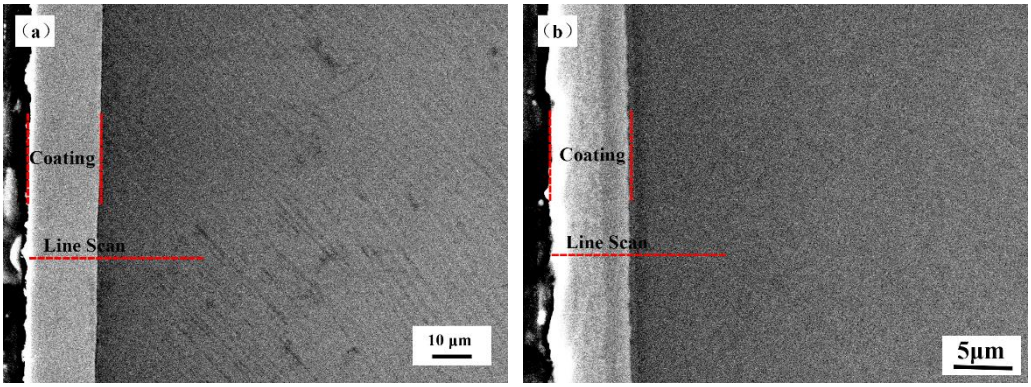

Fig. 4 Cross-sectional SEM morphology of Cr-Nb coated TiAl samples (a) $CrNb_4$, (b) Cr_4Nb.

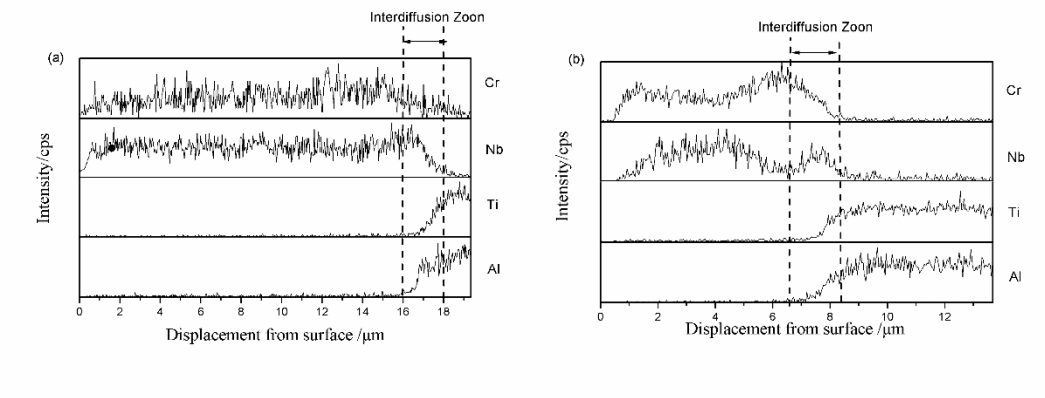

Fig. 5 Line scanning of Cr-Nb coated TiAl samples (a) $CrNb_4$, (b) Cr_4Nb.

3.2 Scratch

Fig. 6 shows the result of the scratch test. Cr-Nb coatings were destroyed gradually with a progressive load from 0 to 50 N. At a certain critical load, the coating would start to fail. The critical load of $CrNb_4$ coating was 17.6 N when that of the Cr_4Nb coating was 21.64 N.

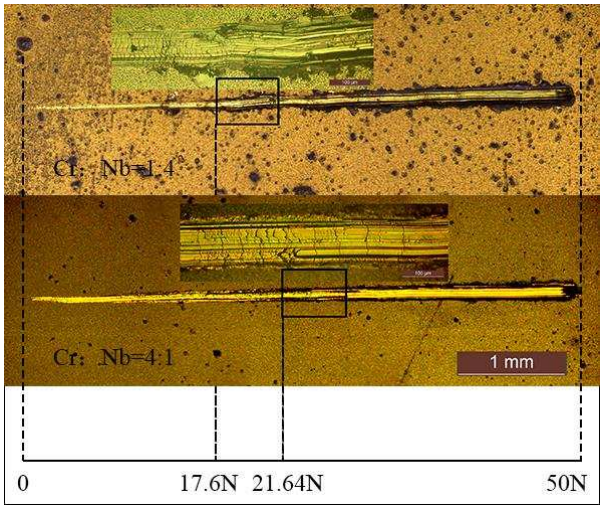

Fig. 6 Optical Microscopy of scratch tracks.

3.3 Nano-indentation

Fig. 7 illustrates typical load-displacement curves of uncoated and Cr-Nb coated TiAl samples in average value, and the values of the hardness and the elastic modulus are shown in Table 3.

It can be seen that the hardness of $CrNb_4$ coating was 11.61GPa and the Cr_4Nb coating was 9.66 GPa which all higher than that of the uncoated TiAl which was 5.65

GPa.

Recently, many researchers have proven that the elastic strain to failure (H/E) and plastic deformation resistance factor (H^3/E^2) should be more suitable than the hardness alone for predicting wear resistance than hardness alone[15]. As showed in Table 3, the H/E and H^3/E^2 value of Cr-Nb coated TiAl samples were all greater than that of the uncoated TiAl which predict good wear resistance.

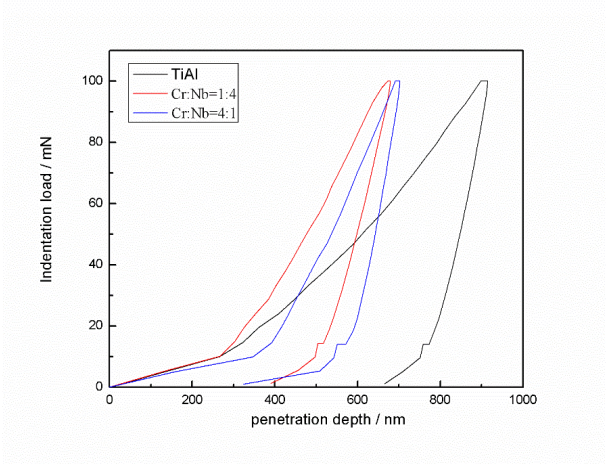

Fig. 7 Load-displacement curves of uncoated and Cr-Nb coated TiAl samples.

Table. 3 The mechanical properties of uncoated and Cr-Nb coated TiAl samples.

Item	Vickers hardness ($HV_{0.1}$)	Hardness (Gpa)	Er (Gpa)	H/E	H^3/E^2
TiAl	209	5.65	167.75	0.0338	0.0064
$CrNb_4$	507	11.61	194.12	0.0598	0.0153
Cr_4Nb	441	9.66	253.68	0.0381	0.0140

3.4 Wear Tests

Fig. 8 shows the friction coefficient of uncoated and Cr-Nb coated TiAl samples conducted at room temperature at a constant angular speed of 10 Hz and a normal load of 4N for 15min. It can be seen that the average friction coefficient of the $CrNb_4$ coating was 0.55 which was the same with the substrate. However, the friction

coefficient curve of the Cr_4Nb coating was more stable and smoother with a higher value ~0.65.

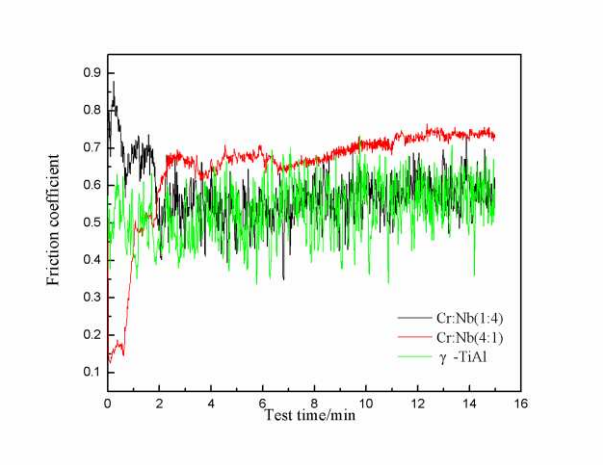

Fig. 8 Friction coefficient

As Fig.9 and Table. 4 showed, the wear track of the $CrNb_4$ coating was much deeper and wider than that of the uncoated TiAl, indicating that the coating was seriously damaged during the course of friction. However, the Cr_4Nb Coating was well preserved with nearly no damage, indicating a good wear resistance. And the specific wear rate of $CrNb_4$ coating, Cr_4Nb coating and uncoated TiAl were 3.54×10^{-4}, 0.01×10^{-4} and $1.53\times10^{-4}mm^3N^{-1}m^{-1}$ respectively.

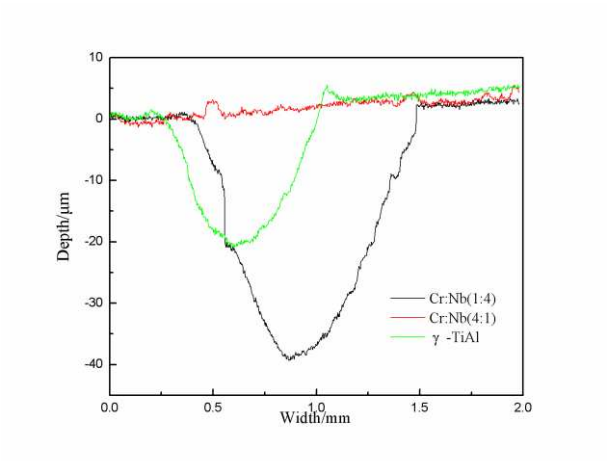

Fig. 9 surface profile curves of uncoated and Cr-Nb coated TiAl samples.

Table. 4 Geometry parameters of wear track for uncoated and Cr-Nb coated TiAl samples.

Items	TiAl	$CrNb_4$	Cr_4Nb
Wear width/mm	0.82	1.09	0.28
Wear depth/μm	22.74	40.01	2.23
Wear volume/mm^3	0.06	0.13	0.01
Wear rate/$10^{-4}mm^3 \cdot m^{-1}$	6.30	14.59	0.02
Special wear rate /$10^{-4}mm^3 \cdot N^{-1} \cdot m^{-1}$	1.53	3.54	0.01

Fig. 10 shows the surface morphologies of wear scar for uncoated and Cr-Nb coated TiAl samples. In Fig. 10(a), that a deep and smooth furrow with no plastic flow was observed clearly in the surface of the uncoated TiAl. In Fig. 10(b), numerous ridges and grooves were presented on the wear scar surface of $CrNb_4$ coating with severe plastic flow and adhesive wear. In Fig. 10(c), it can be seen that the Cr_4Nb coating was well preserved.

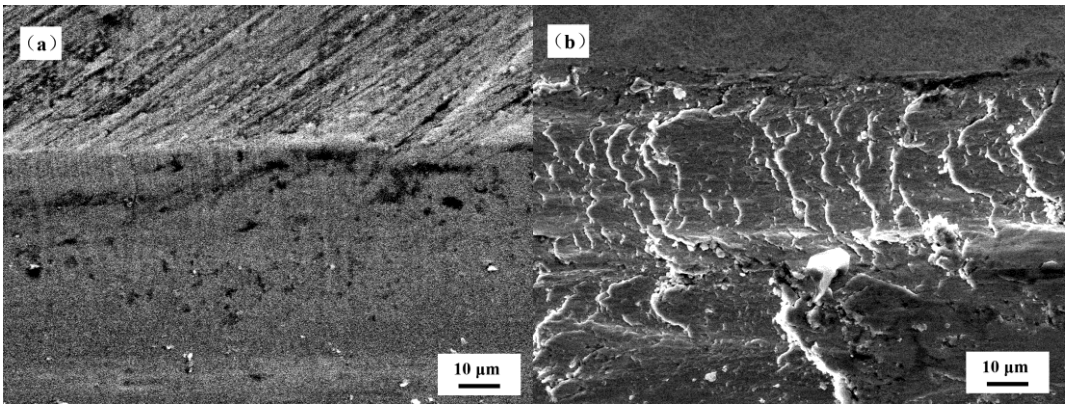

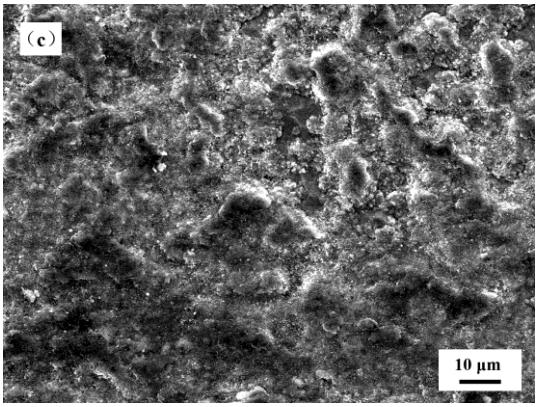

Fig. 10 Surface morphologies of wear scar (a) uncoated TiAl, (b) $CrNb_4$, (c) Cr_4Nb.

4 Discussion

The results showed that Cr-Nb coatings were deposited successfully on the TiAl alloy by the DGP surface alloying technique. The morphology of the Cr-Nb coated Ti-Al samples revealed uniform and compact layers with a little protuberances generated on the surface, which was caused by the growth of sputter atoms cluster in number or quantity and the ion sputter etching happened in specimen surface during the treated process[16].

However, the elements composition of deposited coatings presented in Fig. 2 were different from the sputtering targets. The reasons for such a difference in the composition are that the composition of the deposited coatings is related to not only the composition of targets materials but also the sputtering yields of the various elements of the target materials. Furthermore, the diffusion of different alloying elements at the interface between the as deposited coatings and substrate also affects the final composition of the coatings[14]. Nb is soluble in comparatively large amounts in the γ as well as α_2 phase and has been found to be particularly advantageous for γ(TiAl) engineering alloys[17].

The main phases of the Cr-Nb Ti-Al alloy samples were identified as Cr, Nb and laves Cr_2Nb phase (fig. 3). And as Fig. 11 shown, the assessed Cr-Nb phase diagram, contains only one congruently melting intermediate phase ~Cr_2Nb and this phase forms a eutectic with each of the terminal solid solutions ~ Cr and Nb[18]. Laves Cr-Nb phase with high melting point and moderate density have led to improving mechanical properties

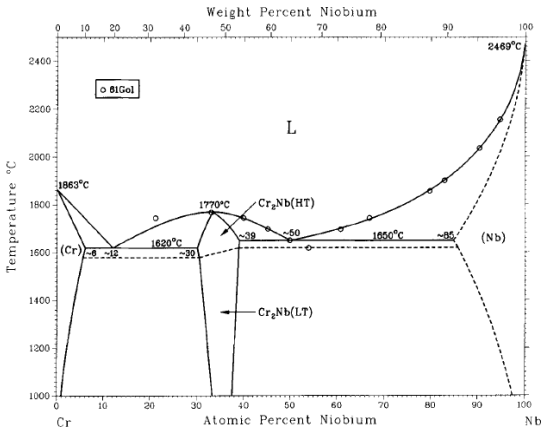

Fig. 11 Cr-Nb phase diagram[18]

Moreover, it can be seen that the thickness of $CrNb_4$ coating was up to 18 μm which was about 2 times than that of the Cr_4Nb ~8 μm (fig. 4 and fig. 5). The thickness of more Nb coating was larger than more Cr coating maybe due to the two reasons, one reason is that Nb element has more sputtering yields than Cr element in the DGP environment. Another is that Nb element is easier solution in TiAl alloy than Cr element[6].

The EDS analysis revealed that Cr and Nb exist in a gradient distribution in the diffusion layer, which was beneficial to the interfacial bonding strength of the coating (fig. 5). And an external diffusion phenomenon of Ti and Al was revealed. Due to the high temperature and the deformation gradient, alloy elements diffuse in the surface layer. But the difference of surface deformation gradient and diffusion coefficient of alloying elements in the surface layer lead to the severe change of concentration gradient in infiltrated layer[19]. It has been reported that the existence of the diffusion layer has remarkable results for improving the performance of combination between the modified layer and TiAl substrate[10, 20, 21].

As fig. 6 shown, microcracks perpendicular to the scratch direction accompanied by chipping of the coatings along the sides of the scratch track were observed when the scratching loads exceed the critical loads that the coatings could support. It is

evident that the critical loads increase with the content of Cr in the coatings. Scratch tests showed that the critical load of Cr_4Nb coating ~21.64 was bigger than that of the $CrNb_4$ coating ~17.6 which indicated a better adhesive properties.

The Nano-indentation tests showed that the hardness of Cr-Nb coated TiAl samples was improved by a significant amount comparing the uncoated TiAl (fig. 7), which may be attributed to the compact structure of the deposited coating. And the hardness of $CrNb_4$ coating ~11.61GPa was higher than that of the Cr_4Nb coating ~9.66 GPa (table 3). There are two strengthening mechanisms of the coating for improving the mechanical properties of the metal alloy: second phase strengthening and solution strengthening[22, 23]. The former is the main way of the coating like PVD, for Cr-Nb coated TiAl alloy, Cr_2Nb is the main second phase with simple Cr phase and Nb phase are few. The latter is diffusion coating, like Ion implantation and DGP surface alloying technique. However, it is proved that Nb element is more soluble in TiAl than Cr element, indicating that the hardness of the $CrNb_4$ coating is bigger than that of the $CrNb_4$ coating.

The wear tests showed that the friction coefficient of TiAl substrate fluctuated strongly by the time (fig. 8), due to the repeated adhesive and tear process during the wear test[24]. And the deep and smooth wear track (fig. 9 and fig. 10(a)) indicated that abrasive wear is the main wear mechanism. For the $CrNb_4$ coating, the friction coefficient was slightly higher and more stable than that of the uncoated TiAl (fig. 8). And severe plastic flow presented on the wear scar (fig. 9 and fig. 10(b)), indicating that adhesive wear is the main wear mechanism, abrasive wear also exists. For the Cr_4Nb coating, adhesive wear is the main wear mechanism. only plastic flow without spalling wear debris presented on the wear scar surface (fig. 9 and fig. 10(c)) due to the good binding force, which resulted in a small loss of wear volume.

5 Conclusions

Cr-Nb coatings were successfully formed onto the TiAl substrate by DGP surface alloying technique, and the coatings were metallurgically bonded to the substrate without defects of porosity or cracks. The main phases of the Cr-Nb coated Ti-Al alloy samples were identified as Cr, Nb and laves Cr_2Nb phase. Moreover, the thickness of the $CrNb_4$ coating was up to 18 μm which was about 1 times higher than that of the Cr_4Nb coating ~8 μm. Scratch tests showed that the critical load of Cr_4Nb coating ~21.64 is bigger than that of the $CrNb_4$ coating ~17.6. Nano-indentation showed the hardness of the $CrNb_4$ coating was 11.61GPa and the Cr_4Nb coating was 9.66 GPa which all larger than that of the uncoated TiAl which was 5.65 GPa. The specific wear rate of the $CrNb_4$ coating, Cr_4Nb coating and uncoated TiAl were 3.54×10^{-4}, 0.01×10^{-4} and $1.53\times10^{-4}mm^3N^{-1}m^{-1}$ respectively. Furthermore, the wear surface analysis shows that for the $CrNb_4$ coating, the friction coefficient was higher and more stable than that of the uncoated TiAl. And severe plastic flow presented on the wear scar, indicating that adhesive wear is the main wear mechanism, abrasive wear also exist; For the Cr_4Nb coating, adhesive wear is the main wear mechanism, only plastic flow without spalling wear debris presented on the wear scar surface due to the good binding force, which resulted in low wear volume.

Acknowledgements

This project was supported by National Natural Science Foundation of China (Grant No. 51175247), Natural Science Foundation for Young Scientists of Jiangsu Province, China (Grant No. BK20140819) and the Priority Academic Program Development of Jiangsu Higher Education Institutions.

Reference

1. E. A. Loria: 'Gamma titanium aluminides as prospective structural materials', Intermetallics, 2000, **8**(9), 1339-1345.

2. K. Kothari, R. Radhakrishnan, and N. M. Wereley: 'Advances in gamma titanium aluminides and their manufacturing techniques', Progress in Aerospace Sciences, 2012, **55**, 1-16.

3. H. Clemens and S. Mayer: 'Design, processing, microstructure, properties, and applications of advanced intermetallic TiAl alloys', Adv. Eng. Mater., 2013, **15**(4), 191-215.

4. H. Baur, R. Joos, W. Smarsly, and H. Clemens: 'γ−TiAl for Aeroengine and Automotive Applications', Intermetallics and Superalloys, 2000, **10**, 384-390.

5. C. Woodward and S. Kajihara: 'Density of thermal vacancies in γ-Ti–Al–M, M= Si, Cr, Nb, Mo, Ta or W', Acta. Mater., 1999, **47**(14), 3793-3798.

6. C. Herzig, T. Przeorski, M. Friesel, F. Hisker, and S. Divinski: 'Tracer solute diffusion of Nb, Zr, Cr, Fe, and Ni in γ-TiAl: effect of preferential site occupation', Intermetallics, 2001, **9**(6), 461-472.

7. R. Yu, L. He, and H. Ye: 'Effect of W on structural stability of TiAl intermetallics and the site preference of W', Phys.Rev. B, 2002, **65**(18), 184102.

8. K. Fujita: 'Research and development of oxidation, wear and corrosion resistant materials at high temperature by surface modification using ion processing', Surf. Coat. Technol., 2005, **196**(1), 139-144.

9. C. Boonruang, T. Thongtem, M. McNallan, and S. Thongtem: 'Effect of nitridation and carburization of γ-TiAl alloys on wear resistance', Mater. Lett., 2004,

58(25), 3175-3181.

10. Z. Xu, X. Liu, P. Zhang, Y. Zhang, G. Zhang, and Z. He: 'Double glow plasma surface alloying and plasma nitriding', Surf. Coat. Technol., 2007, **201**(9), 4822-4825.

11. H. Wu, P. Zhang, J. Li, G. Hussain, and Z. Xu: 'The friction and wear properties of Ti–Al–Nb intermetallics by plasma surface alloying', Tribol. Lett., 2008, **30**(1), 61-67.

12. Z. He, Z. Wang, X. Liu, and P. Han: 'Preparation of TiAl–Cr surface alloy by plasma-surface alloying technique', Vacuum, 2013, **89**, 280-284.

13. Z. Liu, J. Lin, S. Li, and G. Chen: 'Effects of Nb and Al on the microstructures and mechanical properties of high Nb containing TiAl base alloys', Intermetallics, 2002, **10**(7), 653-659.

14. J. Xu, H. Fan, and Z. Li: 'Role of Al additions in wear control of nanocrystalline Mo $(Si_{1-x}Al_x)_2$ coatings prepared by double cathode glow discharge technique', Mater, Sci. Technol., 2013, **29**(8), 900-907.

15. A. Leyland and A. Matthews: 'On the significance of the H/E ratio in wear control: a nanocomposite coating approach to optimised tribological behaviour', Wear, 2000, **246**(1), 1-11.

16. B. Ren, Q. Miao, W. Liang, Z. Yao, and P. Zhang: 'Characteristics of Mo–Cr duplex-alloyed layer on Ti6Al4V by double glow plasma surface metallurgy', Surf, Coat. Technol., 2013, **228**, S206-S209.

17. F. Appel, J. D. H. Paul, and M. Oehring: 'Gamma titanium aluminide alloys: science and technology', 2011, John Wiley & Sons.

18. M. Venkatraman and J. Neumann: 'The Cr-Nb (Chromium-Niobium) system', Bulletin of Alloy Phase Diagrams, 1986, **7**(5), 462-466.

19. K.-Y. Tsai, M.-H. Tsai, and J.-W. Yeh: 'Sluggish diffusion in Co–Cr–Fe–Mn–Ni high-entropy alloys', Acta. Mater., 2013, **61**(13), 4887-4897.

20. L. Duarte, A. Ramos, M. Vieira, F. Viana, M. Vieira, and M. Koçak: 'Solid-state diffusion bonding of gamma-TiAl alloys using Ti/Al thin films as interlayers', Intermetallics, 2006, **14**(10), 1151-1156.

21. M. Goral, L. Swadzba, G. Moskal, G. Jarczyk, and J. Aguilar: 'Diffusion aluminide coatings for TiAl intermetallic turbine blades', Intermetallics, 2011, **19**(5), 744-747.

22. H. Chen and H.-q. Li: 'Microstructure and wear resistance of Fe-based coatings formed by plasma jet surface metallurgy', Mater. Lett., 2006, **60**(11), 1311-1314.

23. X.-T. Luo, G.-J. Yang, and C.-J. Li: 'Multiple strengthening mechanisms of cold-sprayed cBNp/NiCrAl composite coating', Surf. Coat. Technol., 2011, **205**(20), 4808-4813.

24. J. Małecka, W. Grzesik, and A. Hernas: 'An investigation on oxidation wear mechanisms of Ti–46Al–7Nb–0.7 Cr–0.1 Si–0.2 Ni intermetallic-based alloys', Corros. Sci., 2010, **52**(1), 263-272.